Formation of solid solutions of gallium in Fe–Cr and Fe–Co alloys: Mössbauer studies and first-principles calculations

ARTICLE *in* JOURNAL OF ALLOYS AND COMPOUNDS · NOVEMBER 2014

Impact Factor: 3 · DOI: 10.1016/j.jallcom.2014.06.068

9 AUTHORS, INCLUDING:

Oleg I. Gorbatov
Institute of quantum materials science
12 PUBLICATIONS **72** CITATIONS
SEE PROFILE

Yuri Gornostyrev
Institute of quantum materials science
180 PUBLICATIONS **1,117** CITATIONS
SEE PROFILE

Journal of Alloys and Compounds 614 (2014) 297–304

Contents lists available at ScienceDirect

Journal of Alloys and Compounds

journal homepage: www.elsevier.com/locate/jalcom

Formation of solid solutions of gallium in Fe–Cr and Fe–Co alloys: Mössbauer studies and first-principles calculations

V.V. Serikov [a], N.M. Kleinerman [a,*], A.V. Vershinin [a], N.V. Mushnikov [a], A.V. Protasov [a], L.A. Stashkova [a], O.I. Gorbatov [a,b], A.V. Ruban [b], Yu.N. Gornostyrev [a]

[a] Institute of Metal Physics UB RAS, S. Kovalevskaya str. 18, 620990 Ekaterinburg, Russia
[b] Department of Materials Science and Engineering, KTH Royal Institute of Technology, SE - 100 44 Stockholm, Sweden

ARTICLE INFO

Article history:
Received 18 March 2014
Received in revised form 2 June 2014
Accepted 12 June 2014
Available online 20 June 2014

Keywords:
Fe–Cr and Fe–Co alloys
Ga doping
Phase transformations
Mössbauer effect
Density functional theory

ABSTRACT

Investigation of Ga influence on the structure of Fe–Cr and Fe–Co alloys was performed with the use of Mössbauer spectroscopy and X-ray diffraction methods. The experimental results are compared with results of first-principles calculations of the mixing and solubility energies for Ga in an Fe–X (X = Co, Cr) alloy both in ferromagnetic and paramagnetic states. It is shown that Ga mainly goes into the solid solutions of the base alloys. In the alloys of the Fe–Cr system, doping with Ga handicaps the decomposition of solid solutions, observed in the binary alloys, and increases its stability. In the alloys with Co, Ga also favors the uniformity of solid solutions. The results of the first-principles calculations testify in favor of a preferable dissolution of Ga in the FeCo regions of a multicomponent structure rather than FeCr regions, both types of regions being in the ferromagnetic state at the temperature of annealing. The analysis of Mössbauer experiments gives some grounds to conclude that if, owing to liquation, clusterization, or initial stages of phase separation, there exist regions enriched in iron, some amount of Ga atoms prefer to enter the nearest surroundings of iron atoms, thus forming binary Fe–Ga regions (or phases).

1. Introduction

Many research works have recently been devoted to designing and application of hard magnetic materials in which a good combination of magnetic and mechanical properties can be achieved. The majority of hard magnetic materials known, unfortunately, are brittle by origin. However, among the material with medium hard magnetic properties, alloys of the Fe–Cr–Co system can be picked out since, even in series of conventional compositions, they are ductile and workable. These alloys have been subject-matter of studies using different experimental methods for several decades, but the priority in these works has been to ascertain the interrelation of structure and magnetic properties in order to enhance coercivity. It was established [1] that in the high-coercive state, structure of the alloys forms as a result of precipitation hardening of the initial high-temperature homogeneous α-Fe solid solution with the formation of a weak magnetic α_2-phase enriched in FeCr and hard magnetic α_1-phase enriched in FeCo. The redistribution of elements between these components of such a modulated structure occurs in the course of step annealing at temperatures 640–560 °C.

In works of the latest decade, special attention has been paid to enhancement of mechanical characteristics of these alloys. The kinetics of phase separation and final magnetic and mechanical properties of the Fe–Cr–Co alloys largely depend on composition. In recent works, it has been shown that in hard magnetic alloy Fe–22%Cr–15%Co, strength and plasticity can be increased by alloying with tungsten and gallium [2]. Structure investigation showed that in the course of the treatment applied in the structure of the alloy doped with tungsten there appears a disperse phase enriched in tungsten that favorably affects the material strength but increases its brittleness [3]. Additional doping of the alloys with gallium increases plasticity and serves to design hard magnetic alloys with strength properties at a level of those of high-strength structural steels [4,5].

Although the content of Ga in the alloy is small (0.5–3 wt.%), its effect on plastic properties is significant. The mechanism of such influence has not been studied in detail. Yet, a supposition was made that Ga atoms are distributed over the sample bulk inhomogeneously and can plausibly be localized in peripheral regions of precipitates, thus decorating them, which results in the increase

* Corresponding author.
E-mail address: kleinerman@imp.uran.ru (N.M. Kleinerman).

http://dx.doi.org/10.1016/j.jallcom.2014.06.068
0925-8388/

in plasticity [2]. However, the highest plasticity is realized at a concentration of Ga of 0.5% while further increase in the amount of Ga leads to decreasing the relative elongation. The reasons for such a behavior have not been discussed so far. In earlier studies, the alloy structure was represented by three types of regions, namely, η′-phase regions containing W and regions of the α_1- and α_2-type. Against such a background, the presence of small additions of Ga could not be detected.

Gallium alloys are employed in different developments. Its interaction with metals has been studied for over 40 years. Mostly, these researches dealt with compounds of Ga with light or rare-earth metals. Among the alloys with transition metals, in most detail is studied the iron-gallium system, many different methods being used, including Mössbauer spectroscopy [6]. The cobalt-iron alloys also have been the subject-matter of numerous Mössbauer studies, for example [7], but mainly for the concentration range 25–75 at.%. At the same time, for the system Fe–Co–Ga, only three isothermal sections of the phase diagram were reported [8]. Little information is added by the works where vacancy and site occupation [9] and the phase equilibria, A2/B2 and B2/L21 order–disorder transitions, and ferromagnetic/paramagnetic transition on the Co–Fe side [10] of the Co–Fe–Ga Heusler alloy system were examined by different methods, predominantly for high Ga concentrations. The phase diagram of Fe–Cr system is considered to be well studied, and the presence in it of the miscibility gap for α-solid solution was confirmed by different methods. The processes of formation of Fe–Cr phases by the mechanisms of nucleation and spinodal decomposition were studied using Mössbauer method as well [11], but no interest in the influence of Ga on these processes has arisen so far. Thus, the literature data on the structure of alloys of transition metals with Ga are scarce and cannot help clarify the role of Ga in the formation of structure elements in the complex 5-component hard magnetic alloy Fe–Co–Cr–W–Ga.

In the study presented, to gain the information required, the investigation of Ga influence on the structure of model three-component alloys Fe–Cr–Ga and Fe–Co–Ga was performed with the use of Mössbauer spectroscopy and X-ray diffraction. The compositions of the alloys under study were chosen based on the composition of magnetic phases observed in the 5-component hard magnetic alloy Fe–Co–Cr–W–Ga after the heat treatment for optimal magnetic and mechanical properties [2]. Aiming at determination of factors that control the thermodynamics of formation of solid solutions Fe–X–Ga (X = Co, Cr), the first-principles calculation of the mixing and solubility energies for Ga in an Fe–X alloy both in ferromagnetic and paramagnetic states was performed by using density functional theory (DFT) methods and coherent potential approximation (CPA) of electronic structure in alloys.

2. Experimental details

Alloys $(90-x)$Fe–10Cr–xGa, $(85-x)$Fe–15Co–xGa, and $(78-x)$Fe–22Co–xGa, x = 0.5–4 (herefrom, wt%) were melted in an induction furnace in argon atmosphere. Hot-rolled plates were quenched from the temperatures 900, 1050, and 1300 °C, respectively, and then annealed at a temperature of 600 °C for 4 h. The temperature of annealing corresponds to one of the stages of annealing of the multicomponent hard magnetic alloys. Besides, it is just this annealing temperature that was chosen in a number of works devoted to investigation of structure changes in binary Fe–Co and Fe–Cr alloys. Mössbauer spectra were measured at 300 K in the mode of constant accelerations with a source of Co^{57} in the rhodium matrix approximately 900 MBq in activity. Measurements were performed on foils 20 μm thick with the use of an MS1101 spectrometer (512 channels, $(5–8)\times10^5$ counts/channel, the quality factor 70–80). Spectra were analyzed, with account for the effects of self-absorption, using the program package MSTOOLS [12]. Isomer shifts were taken relative to the spectrum of α-Fe.

The structure and phase composition of the alloys were also studied using X-ray diffraction method. The X-ray examination was done on a diffractometer DRON-6 in a monochromotized Cr-Kα radiation. The phase analysis was performed with the use of program packages PowderCell and FullProf.

3. Results and discussion

3.1. Calculation of energies of mixing and solubility of Ga in alloys Fe–Cr and Fe–Co

The exact muffin-tin orbitals (EMTO) method [13] in the framework the density functional theory (DFT) was used to calculate electronic structure and total energies in random bcc Fe–Co–Ga Fe–Cr–Ga alloys. Substitutional disorder in the alloys was treated within the coherent potential approximation (CPA) [14]. The accuracy of the CPA was checked in the corresponding locally self-consistent Green's function calculations and EMTO-LSGF [15,16]. The LSGF method was also used to determine the parameters (screening constants) describing the contributions of screened Coulomb interactions to the one-electron potential, V_i^{scr}, of alloy component i and to the total energy, E_{scr}, within the single-site DFT formalism [17]:

$$V_i^{\mathrm{scr}} = -\alpha_{\mathrm{scr}}\frac{e^2 q_i}{S} \quad \text{and} \quad E_{\mathrm{scr}} = \frac{\beta_{\mathrm{scr}}}{2}\sum_i c_i q_i V_i^{\mathrm{scr}} \tag{1}$$

Here, e is the electron charge, S is the Wigner–Seitz radius, q_i and c_i are the average net charge of the atomic sphere and the concentration for ith alloy component, respectively.

The paramagnetic state is described by a disordered local moment (DLM) model [18,19] in which each alloy component is represented by its spin-up (↑) and spin-down (↓) species, which are assumed to be distributed randomly on the underlying lattice. The total energies were determined in the generalized gradient approximation (GGA) [20] using the full charge density (FCD) formalism [13]. All the self-consistent EMTO-CPA calculations were performed by using an orbital momentum cutoff of $l_{\max}$ = 3 for partial waves. The integration over the Brillouin zone was done using a $25\times25\times25$ grid of **k**-points determined according to the Monkhorst–Pack scheme [21]. The convergence of the results was checked by increasing the **k**-point grid up to $41\times41\times41$ in some calculations. The mixing energy is defined as the difference between the total energy of a random alloy, $E((\mathrm{Fe–X})_{1-x}\mathrm{Ga}_x)$, and the weighed sum of total energies of Ga, E(Ga) and the total energies of the alloy E(Fe–X) (hereafter (Fe–X) denotes the composition of the Fe–Cr or Fe–Co alloy), which are calculated in the same bcc structure:

$$E_{\mathrm{mix}}(x) = E((\mathrm{Fe}-\mathrm{X})_{1-x}\mathrm{Ga}_x) - (1-x)E(\mathrm{Fe}-\mathrm{X}) - xE(\mathrm{Ga}). \tag{2}$$

Fig. 1 shows results of calculation of the mixing energy E_{mix} for alloys $(\mathrm{Fe\text{-}X})_{1-x}\mathrm{Ga}_x$ depending on Ga concentration in the ferromagnetic (FM) and paramagnetic (PM) states. It is seen for the

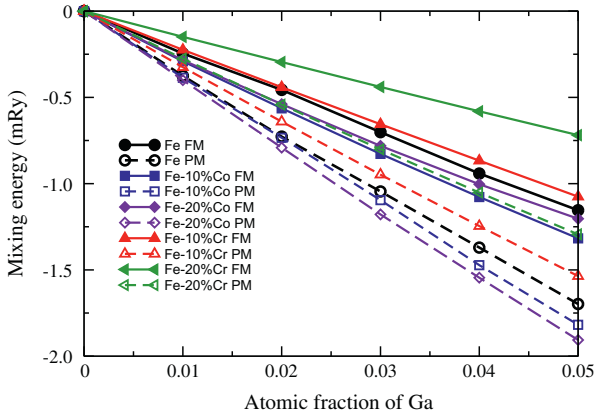

Fig. 1. Dependence of mixing energy calculated for alloys $(\mathrm{Fe}–X)_{1-x}\mathrm{Ga}_x$ on Ga concentration. Solid lines correspond to ferromagnetic state; dashed lines, to paramagnetic state.

alloys under study that Ga enters into a solid solution ($E_{mix} < 0$) both in the case of Fe–Cr and Fe–Co. For a FM Fe–Co–Ga alloy the mixing energy E_{mix} is close to the corresponding value for the Fe–Ga system and only slightly changes depending on Co concentration. At the same time, the energy gain due to the solution of Ga in the FM Fe–20%Cr alloys is approximately two times as small as for Fe–20%Co and it decreases with increasing concentration of X element. For all the compositions, the transition to paramagnetic state is accompanied by increasing the mixing energy and it turns out to be similar for the alloys Fe–(10–20)%Co in the ferromagnetic state and Fe–20%Cr in the paramagnetic state. The above peculiarities manifest themselves when comparing the solution energy

$$E_{sol} = E((\mathrm{Fe} - \mathrm{X})\mathrm{Ga}) - E(\mathrm{Fe} - \mathrm{X}) - E(\mathrm{Ga}) \quad (3)$$

for Ga atom in the Fe–Co and Fe–Cr alloys (see Fig. 2). For a comparison, the energy of dissolution of Ga in pure Fe is found to be 25 mRy for FM state and 38 mRy for PM state, in agreement with previous calculations [22]. As it clearly seen from Fig. 2, the solubility energy is negative and changes gradually with concentration of X element (X = Cr, Co); herewith, the value E_{sol} increases in the case of Fe–Cr alloys and decreases for Fe–Co alloys.

Thus, the results of calculations show that addition of Ga in an amount of up to 5% stabilizes solid solutions Fe–Cr and Fe–Co. Since the solution energy of Ga in Fe–Co alloys and in pure Fe is significantly lower than in Fe–Cr, both being in the ferromagnetic state, it is reasonable to expect that in the Fe–Co–Cr alloys undergoing a spinodal decomposition Ga will preferably enter into regions with enhanced concentration of Fe and Co. This conclusion is valid if the formation of regions enriched in Cr is not accompanied by disordering of magnetic moments. In the opposite case, Ga should be distributed uniformly over the alloy. Evidently, the same regularities can be treated in the case of a complex 5-component hard magnetic alloy Fe–Co–Cr–W–Ga as well.

3.2. Mössbauer and X-ray studies

3.2.1. Alloys (90−x)Fe–10Cr–xGa

Earlier, in studies of the structure of high-strength hard magnetic materials Fe–Cr–Co–W–Ga it was established that unlike conventional compositions Fe–Cr–Co, in multicomponent materials the addition W and Ga results in suppression of the modulated structure formation. However, based on the results of Mössbauer studies, the presence of regions enriched in and depleted of chromium can unambiguously be claimed [2]. Moreover, it was found that changes in the amount of Ga in the alloy mainly affects characteristics of the regions depleted of chromium, whose average concentration was determined to be about 11% [2]. Earlier, in

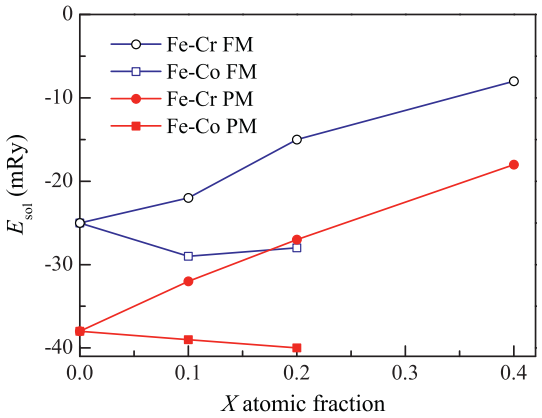

Fig. 2. Solubility energies of Ga in Fe–Cr (circles) and Fe–Co (squares) alloys in FM (open symbols) and PM (solid symbols) states, mRy.

[23] it was established that in binary Fe–Cr alloys with a concentration of chromium less than 15% no decomposition of the solid solution is observed and hyperfine parameters do not depend either on temperature or time of annealing. With this in mind, a concentration of 10% Cr was chosen for the investigation.

Fig. 3a and b shows spectra for the (90−x)Fe–10Cr–xGa alloys in the quenched and annealed states. With increasing Ga concentration, the appearance of the spectra varies. Qualitatively the same changes in the spectra are observed when the content of Cr grows from 10% to 14% [24]. Consequently, the effects of impurity atoms, Cr and Ga, on the spectral form can be taken approximately equal. The corresponding curves of probability-density distribution over hyperfine fields $P(H)$ are given in Fig. 4 which demonstrate that the form of distribution depends on Ga concentration and very poorly varies after annealing. One can pick out a separately resolved peak in high hyperfine fields (H_{hf}) and a set of less resolved peculiarities in lower fields. With increasing concentration of Ga, the position of the high-field peak virtually does not change but its relative intensity falls. Other peaks at lower fields are rather well resolved only for the alloy with 0.5% Ga and at concentrations of Ga 3–4% they nearly merge. As it follows from the data on the dependence of average H_{hf} on Cr content in binary alloys [11], at a concentration less than 15%, the average H_{hf} should not be less than 270 kOe. Theoretical calculations for the disordered state of these compositions give nonzero values for contributions to the spectra from coordinations with 1, 2, and 3 impurity atoms in the nearest neighborhood. Taking into account low Ga concentrations and data on the shift of H_{hf} per Ga atom [6], it should be concluded that the low-intense contributions to $P(H)$ in the field range below 250 kOe are made by possible foreign inclusions in the structure – regions or separate phases significantly enriched in Cr or Ga relative to the composition of the solid solution. Notably, at low Ga amounts, the low-temperature annealing results in an increase of the relative volume fraction of these inclusions, whereas at higher Ga concentrations, they are present already in the quenched state and their fraction does not change upon annealing.

By its appearance, the curve $P(H)$ may purport that already in the state after quenching there starts a separation of the homogeneous solid solution with the formation of regions enriched in and depleted of Cr, with the high-field peak being assigned to the depleted regions. However, to be strict, an analysis of localization of the impurity atoms in the solid solution should be performed. To distinguish contributions to the nearest iron neighborhood from Cr and Ga atoms by solely the H_{hf} values is difficult, taking into account the Mössbauer data for alloys Fe–Cr [11] and Fe–Ga [6]. To this end, the values of isomer shift are needed which for these impurity atoms differ in sign (for Cr atom it is negative, whereas for Ga, positive).

To more definitely describe the structure of the alloys, the spectra were fitted with a number of subspectra with the equal ratio of half-widths for the lines in a subspectrum, taken from the reference spectrum of pure iron. Fig. 5a shows an example of such fitting and in Fig. 5b there are shown correlation dependences of relative intensities of the subspectra on H_{hf} for two concentrations of Ga, 0.5 and 4%. To compare, the calculated values of the binomial distribution of 10% impurity in a binary alloy are shown matching to the H_{hf} shift per Cr atom in the first coordination shell, as is given in [25]. The results of fitting procedure for all alloys under study are shown in Fig. 6 as a correlation of isomer shift with the H_{hf} value for each particular configuration of iron neighborhood. It can be seen that the contributions with high H_{hf} values are characterized by positive isomer shifts, whereas for configurations with low H_{hf} values, the isomer shift is on the main negative. This indicates a nonuniform distribution of impurity Cr and Ga atoms. The positive isomer shift features coordinations containing

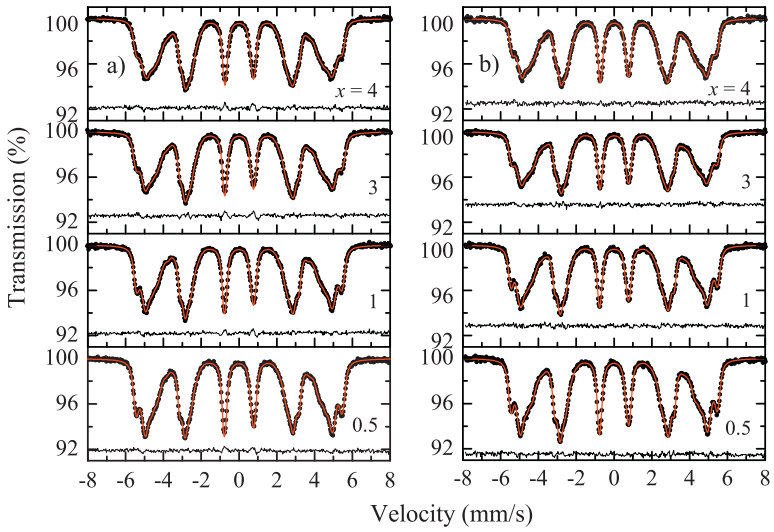

Fig. 3. Mössbauer spectra for alloys Fe–10Cr–*x*Ga with various Ga content *x* in the quenched (a) and annealed (b) states: experiment (symbols) and calculations (red solid lines). Black solid lines in the lower part of each plot show the difference between the experimental and calculated spectra. (For interpretation of the references to color in this figure legend, the reader is referred to the web version of this article.)

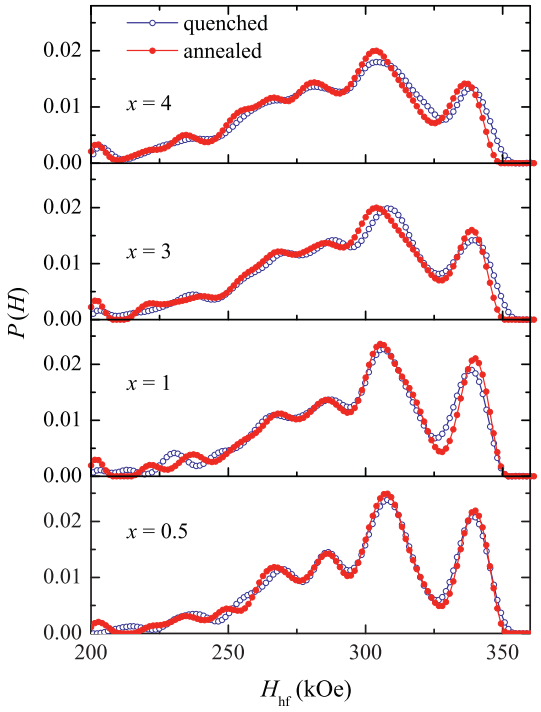

Fig. 4. Probability-density distributions of hyperfine field $P(H)$ for Fe–10Cr–*x*Ga alloys with various *x* in the quenched and annealed states.

predominantly gallium in small amount. Chromium atoms responsible for the negative isomer shift occupy regions with a higher concentration of impurity atoms. From Fig. 6 it is seen that the maximal change of the isomer shift is observed for alloys with smaller concentrations of Ga and after annealing it is even more pronounced. For alloys with 3% and 4% Ga the values of isomer shift are less dependent on the H_{hf} value and remarkably grow after annealing.

If to employ data of [24] gained from the Mössbauer spectra which were measured for the alloys Fe–4%Cr after quenching and annealing at 550 °C, one can compare our data with the isomer shifts determined for main configurations of the neighborhood in nanoclusters. Three contributions with higher fields cannot be ascribed to coordinations Fe:Cr already after quenching. Actually, the contribution with the maximal field H_{hf} = 337 ± 3 kOe would correspond to the configuration FeCr (0,0) in case its isomer shift were 0 mm/c. For the following coordination with one Cr atom, the authors of [24] determined H_{hf} = 308 ± 3 kOe and already negative isomer shift, while in our case, even for samples with the minimal content of Ga, the isomer shift corresponding to these H_{hf} values is positive (Fig. 6). Analogous data for binary Fe–Cr alloys are reported in [23] where changes in H_{hf} and isomer shift per one Cr atom in the first and second coordination shells were determined form the spectra of the alloys subjected to different heat treatments with a Cr content of up to 45%. For a close concentration of Cr 10.2%, $H(0,0) = \sim 342$ kOe. Substitution of one Cr atom for Fe leads to the field change $\Delta H_1 = -33$ kOe for the nearest neighborhood and $\Delta H_2 = -20.5$ kOe for the next- nearest neighborhood. The corresponding values for isomer shifts are IS(0,0) = 0.003 mm/s, $\Delta IS_1 = -0.025$ mm/s, $\Delta IS_2 = -0.008$ mm/s. The presence of a large number of fitting subspectra (Fig. 5) and rather small difference ΔH between the adjacent contributions can be ascribed to an influence of more distant shells, but the change in the sign of the isomer shift is by no means explained in the frame of only model of variation of Cr content.

The results of [6] make it possible to compare our experimental data with the parameters of the Fe–Ga configurations. For the concentrations of Ga 0–4%, the average H_{hf} changes from 330 to 324 kOe, and the shift of H_{hf} per Ga atom in the first, second, and third coordination shells makes up −20, −2, and +4.4 kOe, respectively. The isomer shift per Ga atom in these coordinations changes by +0.036, +0.076, and −0.002 mm/s, respectively. Taking into consideration that the field difference between the nearest lines in the experimental spectra is essentially smaller than ΔH for one Cr atom and somewhat smaller than that for Ga atom in the first coordination shell, the effect of the second and even third coordination shells should be accounted. Then, if to assume an additive influence of the nearest neighbors on the isomer shift of an iron atom, as it was shown in [23], the line with the maximal H_{hf} can be assigned to the configuration with no impurity atoms in the first coordination shell and one chromium and one gallium atom in the second coordination shell. In doing so, the second line with the maximal positive isomer shift and lower field can be assigned to the configuration of neighborhood with one Ga atom in the first coordination shell without Cr atoms within the nearest

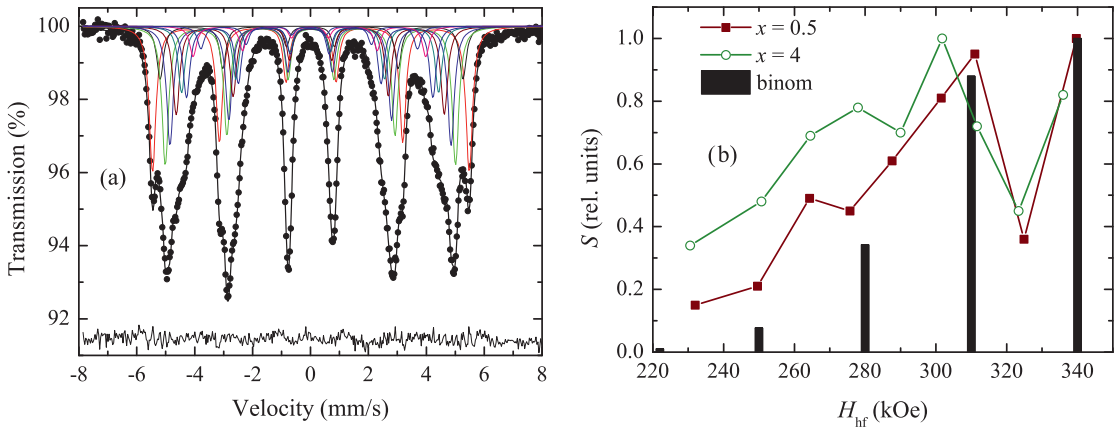

Fig. 5. Example of fitting of Mössbauer spectra for the Fe–10Cr–0.5 Ga alloy with 10 subspectra (a) and correlation plots of relative areas of subspectra versus H_{hf} for the alloys with 0.5% and 4% Ga after annealing (b). Columns show a binomial distribution for 10% amount of impurity atoms.

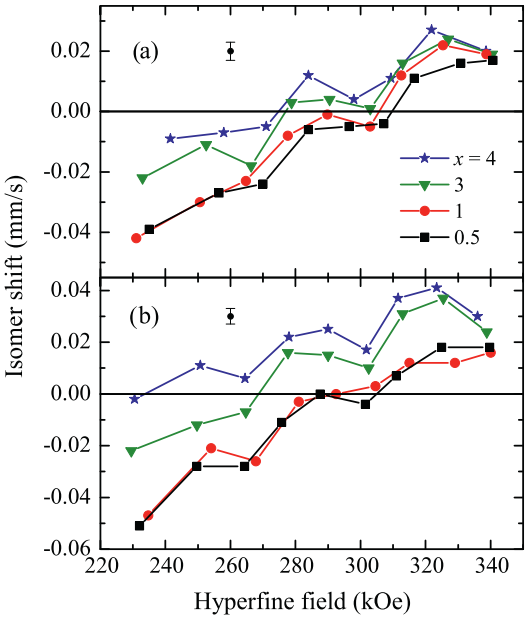

Fig. 6. Correlation of isomer shift with hyperfine field for Fe–10Cr–*x*Ga alloys with various *x* in the quenched (a) and annealed (b) states.

coordination shells. Minding the resemblance of the plots of isomer shift versus H_{hf} for alloys with different Ga content, an assumption can be made that such an arrangement of atoms is characteristic of regions with two or three Cr atoms in the first coordination shell as well.

Thus, in the Fe–Cr alloys studied there takes place the dissolution of Ga atoms in the solid solution after quenching. Although the composition of the binary Fe–10Cr alloy falls in the region of homogeneous solid solution in the phase diagram, the experimental data analyzed indicate a separation of the solid solution in the alloys with (0.5–1% Ga) and formation of the enriched-in and depleted-of Cr regions. Besides, judging by the sign and value of isomer shift, the presence of Ga is evidenced predominantly for the enriched-in-iron regions. If to compare our experimental spectrum for the alloy with 0.5% Ga and the data for the binary alloy with 10% Cr [23], an inference can be made that a liquation of elements is inherent in binary Fe–Cr alloys even for compositions beyond the miscibility gap. As a confirmation, a conclusion of the theoretical work [26] about the formation of clusters in the Fe–Cr alloys with concentrations 10% Cr and more can serve. With growing Ga content in the Fe–Cr–Ga alloys, its distribution tends to be more uniform and the rate of phase separation decreases.

3.2.2. Alloys Fe–Co–Ga

When studying phase transformations in the ternary Co–Fe–Ga, it was shown [8,10] that at a temperature of 1000 °C, in the region of low concentrations of Ga the solid solution possesses an FCC structure and is in paramagnetic state. With decreasing temperature, there takes place a transition into ferromagnetic α (A2) BCC phase which, on further temperature decreasing, transforms into an ordered BCC β (B2) phase at sufficiently high cobalt concentrations.

Publications of Mössbauer study results for such compounds are not available. With accounting for the information on binary Fe–Ga and Fe–Co alloys [6,7], it can be said that the main difficulty in interpreting the experimental data on ternary Fe–Co–Ga alloys consists in the fact that the isomer shift at iron atoms from impurity atoms, both cobalt and gallium, is positive. At the same time, the H_{hf} shifts per impurity atom in the Fe–Co and Fe–Ga alloys are different. Gallium decreases H_{hf} with respect to pure iron, whereas upon alloying with cobalt, it changes nonmonotonously. With increasing Co content in Fe–Co alloys, H_{hf} first increases, reaches its maximum in the vicinity of 25% Co, and further lowers. This causes uncertainty in estimation of the spectral contributions in alloys with high Co concentrations. Besides, possible processes of ordering also can affect the H_{hf} value. Therefore, we studied two series of alloys; with a Co content of 22%, which is close to the composition of the multicomponent Fe–Cr–Co–W–Ga alloys, and that of 15%, which is insufficient for the onset of ordering by either the DO_3 or B2 types.

3.2.2.1. Alloys (85−x)Fe–15Co–xGa. Fig. 7 shows Mössbauer spectra for the 15%Co alloys with a concentration of Ga of 0.5%, 1%, 3%, and 4% in the states after quenching and after annealing at 600 °C for 4 h. The form of spectra and, correspondingly, of distributions shown in Fig. 8 is seen to poorly depend on Ga content and insignificantly changes after annealing. The observed low-intense peak in the distributions $P(H)$ at H_{hf} = 215 kOe may be traceable to the presence of some amount of foreign phases. On the whole, judging by the form of the distribution curve and average H_{hf} value, a conclusion can be made that the material bulk mostly is in the state of solid solution of the specified composition with respect to basic elements. Increasing Ga content leads to a gradual decrease in the intensity of the main peak and growth of an additional peak at a field of 320 kOe, which is close in value to that determined for binary FeGa alloys [6], and then to the appearance of low-intense contributions in a field of about 300 kOe. To estimate compositional

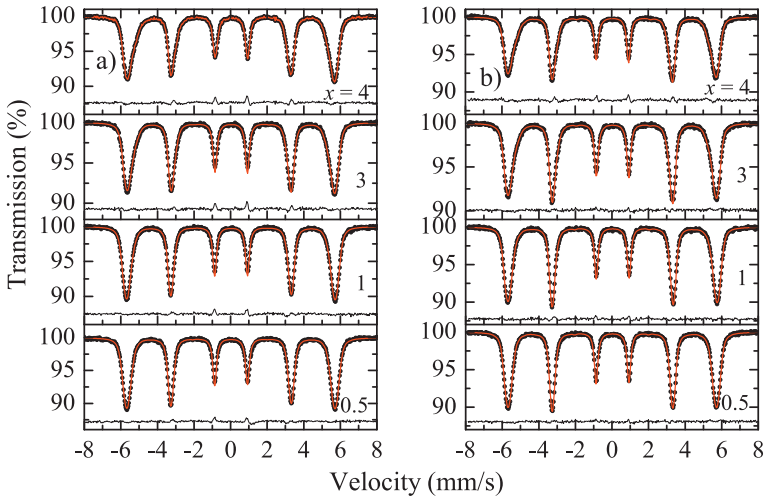

Fig. 7. Mössbauer spectra for alloys Fe–15Co–*x*Ga with various *x* in the quenched (a) and annealed (b) states: experiment (symbols) and calculations (red solid lines). Black solid lines in the lower part of each plot show the difference between the experimental and calculated spectra. (For interpretation of the references to color in this figure legend, the reader is referred to the web version of this article.)

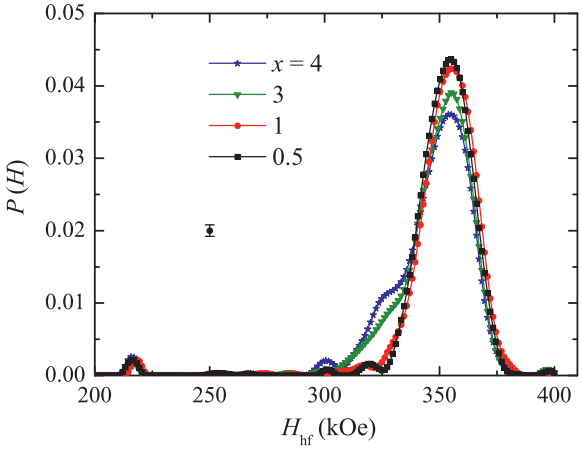

Fig. 8. Probability-density distribution functions of hyperfine field *P*(*H*) for alloys Fe–15Co–*x*Ga with various *x* in the annealed state.

changes, more accurate determination of hyperfine parameters is necessary. Therefore, as the following step, fitting of the spectra with individual subspectra with equal line widths was performed.

In Fig. 9a, normalized histograms show spectral contributions for alloys with different Ga concentrations in the state after annealing. To quantitatively estimate changes in the content of impurity atoms, theoretical values calculated for the binomial distribution of impurity atoms over a generalized coordination shell, which contains 14 atoms in a bcc structure, for the composition $Fe_{85}Co_{15}$ are shown by dashed columns. If to assign the minimal H_{hf} values for the alloy with 0.5% Ga to the coordination of iron neighborhood with no impurity atoms, the other contributions could be ascribed to particular configurations. A comparison of the experimental and calculated values allows a conclusion to be made that addition of 0.5% Ga does not influence the state of the solid solution. A small difference is only observed in the occupancy of the coordination shell with 4 Co atoms. Upon increasing Ga content to 1%, positions of the lines somewhat shift toward low fields, but relative intensities grow for the lines in higher fields. This fact may evidence an increase of the Co content in these regions, with account for changes in the Fe to Co ratio, since gallium was introduced at the expense of iron. In this case, the presence of the peak in a field lower than 330 kOe can be ascribed to regions containing solely Fe and Ga. With further increase in the Ga content to 3% and 4%, shifting of the peaks proceeds further and the relative intensity in lower fields grows, which means that there takes place further mixing of the impurity atoms.

An additional justification of the presence of structure differences in the alloys with low and high Ga contents goes from the isomer shift versus H_{hf} plots shown in Fig 9b. For the composition with 0.5% Ga, the isomer shift is small and virtually equal for all H_{hf} values. In the alloys with higher Ga concentrations, for fields lower than 340 kOe the isomer shift increases up to values that can be explained only be the presence of Ga in the nearest coordination shells. These contributions can be ascribed to the structural regions containing preferably gallium as a second component.

3.2.2.2. Alloys (78−x)Fe–22Co–xGa. The same approach to gaining information from the spectra was employed in the case of alloys with the enhanced concentration of Co as well. The results of fitting are shown in Fig. 10a and b. However, for this compositions, the comparison of experimental and calculated data is already hampered by the necessity for accounting for the effect of the second and third coordination shells, as well as, possible influence, along with the process of ordering, of phase separation similarly to that observed, for example, in FePd even after quenching [27]. Minding the fact that data on the hyperfine parameters for FeCo alloys of compositions close to 20%Co are lacking in literature, we measured a spectrum for the quenched binary alloy $Fe_{80}Co_{20}$ and showed the results of fitting with dashed columns. The positions and intensity of lines for the alloy with 0.5% Ga are seen to be close to those for the binary alloy. The only difference in the intensity of the highest-field line, which, according to the NMR data [28] should be assigned to the third coordination shell, is likely to be related to the predominant occupation of the first and second coordination shells in the case of the alloy with Ga. The tendencies in the behavior of the relative intensities of the spectral contributions with increasing Ga content coincide with the above described for the alloys with the lower Co concentration. No signs of ordering, which develops in binary Fe–22Co alloys after annealing below the Kurnakov temperature ($T = 700\,^{\circ}C$) are observed.

The appearance of the contribution in a field of ~310 kOe indicates the presence of a coordination with an enhanced content of Ga, which in turn purports that in the case of ternary alloys with 22%Co the relative fraction of regions containing Ga is increased.

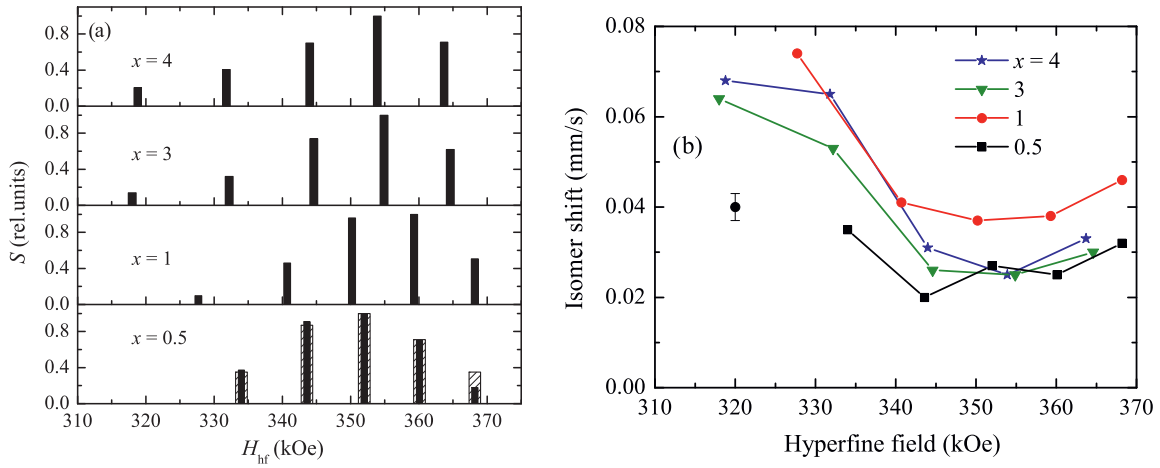

Fig. 9. Histograms of subspectral contributions (a) and isomer shift (b) for individual configurations of iron neighborhood for Fe–15Co–*x*Ga alloys with various *x* in the annealed state. Dashed columns (a) show a binomial distribution for composition Fe–15Co.

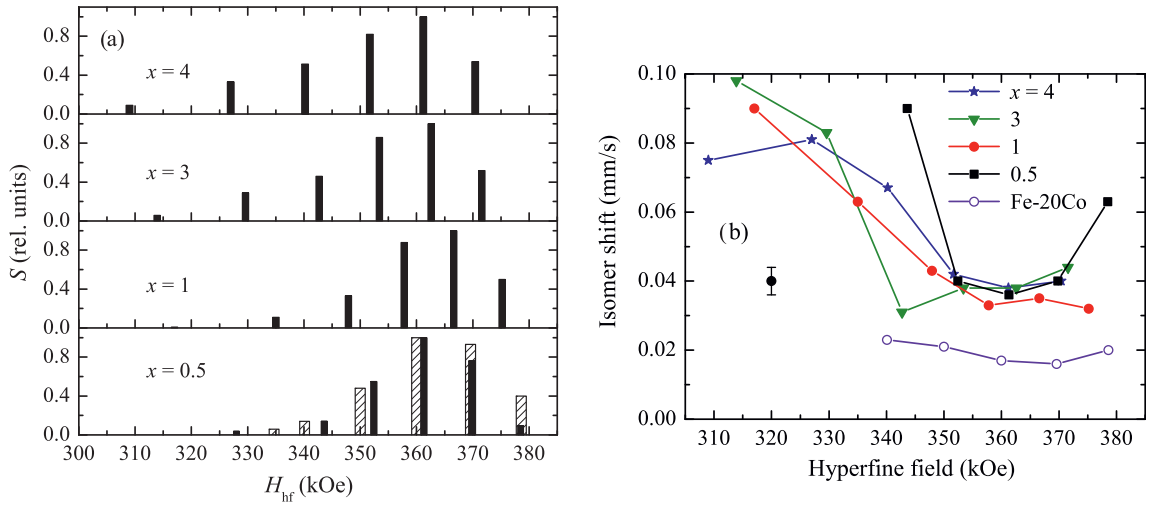

Fig. 10. Histograms of subspectral contributions (a) and isomer shift (b) for individual configurations of iron neighborhood for Fe–22Co–*x*Ga alloys with various *x* in the annealed state. Dashed columns show experimental results for Fe–20Co alloy in the quenched state.

Since the intensities of these contributions are low, the error in their determination grows; however, a qualitative pattern of changes with increasing Ga content (Fig. 10b) and, the more, quantitative comparison with the data for the binary alloy decisively testify to the presence of regions enriched in Ga.

Since the above reasonings following from the analysis of the Mössbauer data proper can by no means characterize macrostructure of the objects under study, additional studies of the changes in the phase composition and morphology of the alloys under study upon their doping with Ga have been conducted.

3.2.3. Results of X-ray investigation

X-ray analysis showed that the samples of alloys (90–*x*)Fe–10Cr–xGa ($0 \leqslant x \leqslant 4$) after quenching from 900 °C contain mainly α-Fe-based solid solution. The low-temperature annealing does not change the structure of the solid solutions. The concentration dependence of the lattice parameter *a* is shown in Fig. 11, which demonstrates a linear growth of the parameter with Ga content. To compare, the similar growth of the lattice parameter observed for the binary Fe–Ga alloy [29] is shown as well. Along with the main phase, in all alloys there is present a 1%–1.5% fraction of a solid solution with an increased lattice parameter, the parameter of this additional phase growing with increasing Ga content from 2.887 to 2.891 Å for $x = 0.5$ and $x = 4$, respectively.

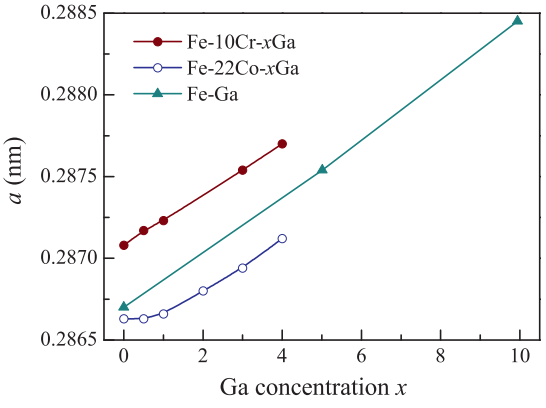

Fig. 11. Concentration dependences of the lattice parameters of ternary alloys Fe–10Cr–xGa and Fe–22Co–xGa ($0 \leqslant x \leqslant 4$) after quenching and annealing and of the lattice parameter for binary Fe–Ga alloys according to data of Ref. [29].

In the alloys Fe–22Co–xGa ($0 \leqslant x \leqslant 4$) after quenching from 1300 °C the main phase is also α-Fe based solid solution. However, with increasing Ga content from 0% to 1%, the parameter *a* virtually

does not change; the linear growth is observed on changing amount of Ga from 1% to 4%. (see Fig. 10). These data agree with the conclusion made based on the results of the Mössbauer studies that introduction of 0.5% Ga into Fe–Co alloys does not affect the state of the solid solution. Along with the main phase, in these alloys, about 2% of an α-Fe based solution with the increased lattice parameter is present as well.

Thus, on the whole, the results of the phase analysis support the conclusions made based on the analysis of the Mössbauer spectra on the state of the solid solutions and behavior of low additions of Ga into the Fe–Cr and Fe–Co alloys. More detailed analysis of the phase composition and morphology of the alloys under study will further be presented elsewhere.

4. Conclusion

The research performed on the fine structure of the quasibinary alloys Fe–10Cr–xGa, Fe–15Co–xGa, and Fe–22Co–xGa has shown that Ga mainly goes into the solid solutions of the base alloys. In the alloys of the system Fe-Cr it handicaps the phase separation of solid solutions, observed in the binary alloys, i.e., makes them more homogeneous. In the alloys with Co, the low amount of Ga does not manifest itself in the structure of the quasibinary alloys. With growth of its concentration, judging by the absence of the signs of ordering, Ga also favors uniformity of the Fe–Co solid solution. Besides, the formation of regions enriched in Ga is observed. The results of the first-principles calculations testify in favor of a preferable dissolution of Ga in the FeCo regions of a multicomponent structure rather than FeCr regions, both types of regions being in the ferromagnetic state at the temperature of annealing. Besides, the analysis of Mössbauer experiments gives some grounds to conclude that if owing to liquation, clusterization, or initial stages of phase separation there exist regions enriched in iron, some amount of Ga atoms prefer to enter the nearest surroundings of iron atoms (in agreement with the results of calculation of the energy of dissolution of Ga in pure Fe), thus forming binary Fe–Ga regions (or phases). The formation of such regions may favorably influence plasticity of multicomponent alloys. More convincing conclusions with allowance for these features can be made in further studies of these objects with structure methods.

Acknowledgements

The work was carried out using facilities of the Center of Collective Use, IMP UB RAS and has been partially supported by Program of UB RAS, Project No. 12-P-23-2005.

References

[1] H. Kaneko, M. Homma, K. Nakamura, M. Okada, G. Thomas, IEEE Trans. Magn. 12 (1977) 1325.
[2] G.V. Ivanova, N.N. Shchegoleva, V.V. Serikov, N.M. Kleinerman, E.V. Belozerov, M.A. Uimin, V.S. Gaviko, N.V. Mushnikov, Phys. Met. Metallogr. 109 (2010) 438.
[3] G.V. Ivanova, N.N. Shchegoleva, V.V. Serikov, N.M. Kleinerman, E.V. Belozerov, J. Alloys Comp. 509 (2011) 1809.
[4] E.V. Belozerov, G.V. Ivanova, N.N. Shchegoleva, V.V. Serikov, N.M. Kleinerman, A.V. Vershinin, V.S. Gaviko, N.V. Mushnikov, Phys. Met. Metallogr. 113 (2012) 312.
[5] E.V. Belozerov, N.V. Mushnikov, G.V. Ivanova, N.N. Shchegoleva, V.V. Serikov, N.M. Kleinerman, A.V. Vershinin, M.A. Uimin, Phys. Met. Metallogr. 109 (2012) 319.
[6] A. Błachowski, K. Ruebenbauer, J. Zukrowski, J. Przewoznik, J. Alloys Comp. 455 (2008) 47.
[7] J.E. Frackowiak, Hyperfine Interact. 60 (1990) 757.
[8] V. Raghavan, J. Phase Equilib. Diffusion 29 (2008) 438.
[9] G.L. Whittle, P.E. Clark, R. Cywinski, J. Phys. F: Met. Phys. 10 (1980) 2093.
[10] R. Ducher, R. Kainum, I. Ohnuma, K. Ishida, J. Alloys Comp. 437 (2007) 93.
[11] J. Cieslak, S.M. Dubiel, B. Sepiol, J. Phys.: Condens. Matter 12 (2000) 6709.
[12] V.S. Rusakov, Mössbauer Spectroscopy for Locally Heterogeneous Systems. Almaty, 2000 (in Russian).
[13] L. Vitos, Computational Quantum Mechanics for Materials Engineers, Springer-Verlag, London, 2007.
[14] P. Soven, Phys. Rev. 156 (1967) 809;
B.L. Gyorffy, Phys. Rev. B 5 (1972) 2382.
[15] I.A. Abrikosov, S.I. Simak, B. Johansson, A.V. Ruban, H.L. Skriver, Phys. Rev. B 56 (1997) 9319.
[16] O.E. Peil, A.V. Ruban, B. Johansson, Phys. Rev. B 85 (2012) 165140.
[17] A.V. Ruban, H.L. Skriver, Phys. Rev. B 66 (2002) 024201;
A.V. Ruban, S.I. Simak, P.A. Korzhavyi, H.L. Skriver, Phys. Rev. B 66 (2002) 024202.
[18] B.L. Gyorffy, A.J. Pindor, G.M. Stocks, H. Winter, J. Magn. Magn. Mater. 45 (1984) 15.
[19] B.L. Gyorffy, A.J. Pindor, J.B. Staunton, G.M. Stocks, H. Winter, J. Phys. F: Met. Phys. 15 (1985) 1337.
[20] J.P. Perdew, K. Burke, M. Ernzerhof, Phys. Rev. Lett. 77 (1996) 3865.
[21] H.J. Monkhorst, J.D. Pack, Phys. Rev. B 13 (1972) 5188.
[22] M.V. Petrik, O.I. Gorbatov, Yu.N. Gornostyrev, Phys. Met. Metallogr. 114 (2013) 885.
[23] S.M. Dubiel, J. Zukrowski, J. Magn. Magn. Mater. 23 (1981) 214.
[24] S.M. Dubel, K. Krop, J. Phys. 12 (1974) C6–459.
[25] S.A. Gerasimov, A.A. Novakova, V.S. Kraposhin, P.V. Bochvarov, Sci. Educ. 48211 (2012) (in Russian).
[26] M.Yu. Lavrentiev, R. Drautz, D. Nguyen-Manh, T.P.C. Klaver, S.L. Dudarev, Phys. Rev. B 75 (2007) 014208.
[27] N.I. Vlasova, N.M. Kleinerman, V.V. Serikov, A.G. Popov, J. Alloys Comp. 583 (2014) 191.
[28] C. Dasarathy, W. Hume-Rothery, Proc. Royal Soc. London. Ser. A, Math. Phys. Sci. 286 (1965) 141.
[29] V. Pierron-Bohnes, M.C. Cadeville, F. Gautier, J. Phys. F: Met. Phys. 13 (1983) 1689.